Microchemical Journal 172 (2022) 106939

Contents lists available at ScienceDirect

Microchemical Journal

journal homepage: www.elsevier.com/locate/microc

Rapid and sensitivity determination of macrolides antibiotics using disposable electrochemical sensor based on Super P carbon black and chitosan composite

William Barros Veloso [a], Anny Thalia de Freitas Oliveira Almeida [b], Lara Kelly Ribeiro [c], Marcelo de Assis [c], Elson Longo [c], Marco Aurélio Suller Garcia [a], Auro Atsushi Tanaka [a,d], Iranaldo Santos da Silva [b], Luiza Maria Ferreira Dantas [b,*]

[a] Departamento de Química, Centro de Ciências Exatas e Tecnologia, Universidade Federal do Maranhão, 65080-805 São Luís, MA, Brazil
[b] Departamento de Tecnologia Química, Centro de Ciências Exatas e Tecnologia, Universidade Federal do Maranhão, 65080-805 São Luís, MA, Brazil
[c] Departamento de Química, CDMF-UFSCar, Universidade Federal de São Carlos, 13565-905 São Carlos, SP, Brazil
[d] Instituto Nacional de Ciência e Tecnologia de Bioanalítica, Caixa Postal 6154, CEP 13083-970, Campinas, SP, Brazil

ARTICLE INFO

Keywords:
Macrolides
Carbon black
super P
Electrochemical sensor
Batch injection analysis

ABSTRACT

Antibiotics in water bodies have raised global concerns due to the risk of developing drug-resistant bacteria stains. Thus, the occurrence of macrolide antibiotic residues in environmental waters has attracted significant attention lately. Herein, a composite material comprised of Super P carbon black particles and chitosan was developed as an electrochemical sensor to determine macrolide antibiotics, including erythromycin, azithromycin, clarithromycin, and roxithromycin. The electrode was characterized by cyclic voltammetry, electrochemical impedance spectroscopy, scanning electron microscopy, and Raman spectroscopy. The proposed sensor coupled to a batch injection analysis system proved to be rapid (125 injections h^{-1}), reproducible (RSD = 2.60%), and present a wide linear range (1.0–190.0 μmol L^{-1}). Also, it was successfully applied for the direct determination of the four macrolide antibiotics in water and pharmaceutical samples. Recovery tests were performed on both samples, in which recovery values between 96.0% and 104.7% were achieved for tests performed on environmental samples, and between 95.6% and 105.1% for tests performed on pharmaceutical samples, proving the excellent accuracy of the system. Based on electrochemical/physicochemical characterizations and sensing performance, the applicability of this material was demonstrated as an attractive alternative for use in routine analysis from economic and portability points of view.

1. Introduction

Macrolides have been categorized as a critically important class of broad-spectrum antibiotics that effectively treat infectious diseases caused by gram-positive and gram-negative bacterias. The antimicrobial effect of macrolides is based on blocking the activity of peptidyl t-RNA on the 50S ribosome, inhibiting protein synthesis during bacterial replication [1,2]. Erythromycin (ERY) was the first macrolide antibiotic to be identified and present clinical applications, from which Azithromycin (AZI), Clarithromycin (CLA), and Roxithromycin (ROX) were synthesized through small structural changes (Fig. 1) [3]. These compounds are widely used in the treatment of infectious diseases as they are active against most infections, especially in the respiratory tract, and can act against atypical respiratory pathogens. Owing to their efficiency and low cost, they are often used in human and veterinary medicine, treating and preventing diseases [4].

The indiscriminate use of these drugs worldwide has been causing severe effects to the environment and, consequently, to the living beings, since 30%–90% of macrolide antibiotics are eliminated intact (non-metabolized) through urine and feces [5,6]. Recent studies have detected macrolide antibiotics in surface waters, sediments, and river and lake biota [7,8]. Therefore, the frequent exposure of aquatic microorganisms to these antibiotics can lead to another significant problem: the emergence of resistant bacteria. As they represent a threat to the environment, a report produced by the European Commission in 2015 includes the macrolide antibiotics ERI, AZI, and CLA in a list that contains the ten substances

* Corresponding author.
E-mail address: luiza.dantas@ufma.br (L.M.F. Dantas).

https://doi.org/10.1016/j.microc.2021.106939
Received 5 August 2021; Received in revised form 18 October 2021; Accepted 20 October 2021
Available online 25 October 2021

potentially harmful to the environment and that require better control [9]. Thus, the importance of analytical methods in monitoring these compounds in the environmental samples becomes evident.

Some analytical methods are reported in the literature for the determination of macrolides, e.g., spectrophotometric [10], capillary electrophoresis [11], and chromatographic methods [12,13]. Liquid chromatography-mass spectrometry (LC-MS) is the most used technique for quantifying macrolide antibiotics in environmental and pharmaceutical samples [13]. This technique has high sensitivity, selectivity, accuracy and presents the possibility of simultaneous determination of several species in a single analysis. However, they require strict sample treatment and pre-concentration steps, generating large amounts of toxic waste. Also, the instrumentation is expensive, and analyzes must be performed in a laboratory without the possibility of fieldwork [14].

Therefore, electrochemical methods are an attractive alternative for the efficient and straightforward determination of pharmaceutical compounds in various sample matrices [15,16]. These methods generally do not require prior sample treatment, and when necessary, they are performed effortlessly, with low-cost instrumentation compared to chromatographic methods. When electrochemical methods are associated with hydrodynamic systems, such as Batch Injection Analysis (BIA), the gain in speed and efficiency is notorious; also, the use of screen-printed electrodes (SPE's) promote the portability of this method, facilitating the analysis under environmental conditions at the sample collection site [17,18]. The modification of working electrodes is widely explored in electrochemical methods to achieve greater sensitivity, stability, and low limit of detection (LOD) and quantification (LOQ). Modifiers based on gold nanoparticles [19], graphene oxides [20], and composites based on molecularly imprinted polymers (MIP's) with metallic nanoparticles and carbon nanotubes were used recently to improve the analytical performance of electrochemical sensors in the detection of antibiotics, increasing the number of electroactive sites and improving the electronic transfer rate at the electrode/solution interface [21,22].

Carbon nanostructures are always an excellent choice to improve the performance of electrochemical sensors. In the light of this, films based on carbon black (CB) nanoparticles have increased relevance as modifiers for electrodes [23–25]. CB is a low-cost amorphous carbon (approximately 1 euro/Kg) formed by roughly spherical particles, produced from incomplete carbon burning or through the pyrolysis of carbonaceous materials in the industry [25,26]. From an electrochemical point of view, CB has desirable characteristics such as high surface area, chemical stability, high conductivity, and the ability to form stable dispersions [25]. Silva and collaborators recently used a film based on CB (Vulcan XC72R) and chitosan to determine the antihypertensive losartan in pharmaceutical compounds and synthetic biological fluids [27]. The sensor was stable and reproducible, with a wide linear range and limit of detection less than 1.0 μmol L^{-1}.

Herein, we present a simple, rapid, versatile, and low-cost method for the determination of ERY and its derivatives AZI, CLA and ROX, in environmental and pharmaceutical samples, using carbon electrodes modified with Super P carbon black film (SPCB) and chitosan (CT), coupled to a batch injection analysis system with amperometric detection (BIA-AMP). To fulfill the demand for a low-cost, compact, and easy-to-use device, the proposed method additionally takes advantage of the reduced size of screen-printed electrodes and the CB electrochemical capabilities. A study of the voltammetric behavior of the prototype macrolide ERY on the modifying film, optimization of all experimental parameters, and application of the method was carried out. Also, electrochemical/physicochemical characterizations were performed, supporting the sensing performance.

2. Experimental

2.1. Reagents e solutions

Deionized water (resistivity ≥ 18 MΩ cm^{-1}) was obtained from a Milli-Q system (Millipore, Bedford, MA, USA) and used to prepare all the solutions. Also, all the reagents were of analytical grade and used as received. The reagents ERY, AZI, CLA, and ROX were purchased from Sigma Aldrich, and the solutions were prepared one day before the experiments. The solvent mixtures used for the antibiotics solutions preparation comprised ethanol:deionized water (v/v) at different ratios: 50:50 (ERY), 70:30 (AZI and CLA), and 80:20 (ROX). For improved dilution, an ultrasonic bath was used for 5 min. Britton-Robinson (BR) buffer solution, used as a supporting electrolyte in the initial voltammetric measurements, was prepared from stock solutions containing acetic acid (Merck, Darmstadt, Germany), phosphoric acid, and boric acid (Isofar, Duque de Caxias, Brazil), 0.1 mol L^{-1} each. 2.0 mol L^{-1} NaOH solution (Isofar, Duque de Caxias, Brazil) was added for pH adjustment. Sörensen buffer solution, used as a supporting electrolyte in amperometric measurements, was prepared from a mixture of 0.1 mol L^{-1} Na_2HPO_4 and KH_2PO_4 stock solutions in the ideal proportion for the required pH value. [28].

2.2. Instrumentation

Cyclic voltammetry (CV) and amperometry (AMP) measurements were performed using an Ivium CompactStat.h portable potentiostat (Ivium Technologies, Eindhoven, Netherlands) connected in a computer equipped with IviumSoft software (version 2.783). Electrochemical Impedance Spectroscopy (EIS) measurements were performed using a FRA2 module coupled to an Autolab PGSTAT 302 N potentiostat/galvanostat (Metrohm Autolab B.V., Utrecht, Netherlands) interfaced to a computer equipped with NOVA software (version 2.1.4). A system composed of a glass electrochemical cell (15 mL) and a Teflon® cap, adapted to accommodate three electrodes, was used in the initial CV and EIS measurements. We used a glassy carbon (GCE, 3.0 mm in diameter), an Ag/AgCl, $KCl_{(sat.)}$, and a platinum wire as working, reference, and counter electrodes, respectively.

BIA-AMP measurements were performed in a system similar to that described by Cardoso et al. [29]. The BIA cell consisted of a cylindrical container with a maximum capacity of 100 mL, produced in a 3D printer using an ABS filament (Acrylonitrile Butadiene Styrene) by the Fused Deposition Modeling (FDM) technique. A single channel EDP3-Pus electronic micropipette (Raynin, MA, USA) was used to inject standard solutions and samples in the upper part of the cell. At the bottom of the cell, a compartment accommodated the screen-printed electrodes (SPEs) (Dropsens, Oviedo, Spain), which remained in contact with the electrolyte solution through a hole. An "O-ring" was used to limit contact with the region of the three electrodes: work, auxiliary, and pseudo-reference (PRE) electrodes.

2.3. Preparation of the modified electrodes

The method for obtaining the electrode modifier was based on the literature, with modifications [25,27]. In a typical procedure, the CB powder was dispersed in 300 μL of dimethylformamide before adding 400 μL of 0.1% chitosan solution (prepared in 1.0% acetic acid) and 300 μL of deionized water. This mixture was maintained under sonication at 59 kHz for 120 min.

Before each modification, the glassy carbon electrode (GCE) and SPEs surface were carefully cleaned. GCE was polished on abrasive paper and synthetic diamond suspension (Kemet, China), followed by rinsing with deionized water. The SPEs were only cleaned with light jets of deionized water before each modification. The electrodes were modified using the drop-casting method, i.e., by adding on the surface of the working electrode 10 μL of the CB dispersion in two successive steps of 5 μL. After each step, the electrodes remained under an airflow at a moderate temperature (around 34 °C) for 10 min or the time necessary for solvent evaporation and film formation. After the modification, the GCE and SPEs were called SPCB-CT/GCE and SPCB-CT/SPE, respectively.

2.4. Physical characterizations

The samples for microscopy analyzes were prepared by drop-casting an isopropanol suspension of the materials over a carbon-coated copper grid, followed by drying under ambient conditions. Field-strength scanning electron microscopy (FEG-SEM) images were obtained using JEOL® JSM-IT300 (JEOL, Tokyo, Japan), operating at 5 kV. The particles sizes range of SPCB was determined using the open-source image processing program ImageJ. Raman spectroscopy was recorded with a micro-spectrometer model LabRAM (Horiba, Tokyo, Japan) at room temperature in the 200–4000 cm^{-1} region using a He-Ne laser as the excitation source through an Olympus TM BX41 microscope operating at a wavelength of 512 nm and maximum output power of 5.9 mW.

2.5. Water and drug samples

Water samples were collected from a lagoon located in the Federal University of Maranhão (São Luís, Maranhão, Brazil). After collection, samples were stored in the absence of light and at 4 °C until usage. Analyzes were performed without any previous sample treatment, with only a dilution in support electrolyte (1:5 v/v). Some samples were enriched with antibiotic standards at different concentrations to perform addition and recovery tests. Drug samples containing AZI and CLA were purchased at a local drugstore and were analyzed using the proposed methodology. Three capsules of each drug were weighed, macerated, and the average mass of a single capsule was determined. Then, these drug masses were dissolved in 100 mL of ethanol:water mixture (70:30 v/v), which was kept in an ultrasonic bath for 20 min for complete solubilization of the analytes; the insoluble excipients were removed by simple filtration, obtaining a clear stock solution.

2.6. Analytical procedures

A preliminary voltammetric study was conducted to prove the electroactivity of ERY and compare the analytical signals between GCE and SPCB-CT/GCE. These measurements were performed in the absence and presence of 40.0 μmol L^{-1} of ERY in an electrochemical cell containing 0.1 mol L^{-1} of BR buffer (pH 7.0). After that, other optimization steps of experimental parameters were carried out to obtain a better analytical response. Thus, the modifier parameters (CB concentration and dispersion volume) and the supporting electrolyte (composition, concentration, and pH) were evaluated. These parameters were used in a portable BIA-AMP system, in which the working potential, injection volume, and dispensing rate of the electronic micropipette were also optimized. Intra ($n = 25$) and inter-day ($n = 10$) repeatability studies were performed to assess the proposed method's precision. The calibration curves for ERY, AZI, CLA, and ROX were obtained by successive injections ($n = 3$) of standard solutions of each antibiotic in the BIA cell containing 50 mL of the supporting electrolyte. LOD and LOQ values were obtained following IUPAC recommendations [30] using the following equations:

$$3 \times SDb/m(\mathrm{LOD})$$

$$10 \times SDb/m(\mathrm{LOQ})$$

where SD_b is the standard deviation of ten measurements of the blank solution (supporting electrolyte only) and m is the analytical sensitivity.

The Randles–Ševćik equation was used to estimate the electroactive surface area of studied working electrodes: [31]

$$I_p = 2.686x10^5 n^{3/2} A C D^{1/2} v^{1/2}$$

where D = 7.6 × 10^{-6} cm^2 s^{-1}, $n = 1$, C = 1.0 × 10^{-6} mol cm^{-3}.

The number of transferred electrons (n) in the ERY oxidation was obtained from the equation:

Ep − Ep/2 = 47.7mV/α.nADDINCSL_CITATION{"citationItems":[{"id":"ITEM − 1","itemData":{"DOI":"10.1007/s10008 − 020 − 04541 − 1","ISSN":"14330768","abstract":"Anovelelectrochemicalmethodfordeterminationofosartanusingaglassycarbonelectrodemodifiedwithcarbonblacknanoparticlesimmobilizedwithinacrosslinkedchitosanfilmisproposed. Theelectrochemicalbehaviorofosartanwasinvestigatedusingcyclicvoltammetry, whichpresentedanirreversibleoxidationpeakatapotentialof + 1.28Vvs.Ag/AgCl(3.0molL − 1KCl).Theelectroactivityofosartanonthemodifiedelectrodewassignificantlyimprovedintermsofpeakpotentialandpeakcurrentintensitycomparativelytobareworkingelectrode.Usingsquare − wavevoltammetrytechniqueunderoptimizedconditions, themodifiedelectrodeshowedalinearresponseintheconcentrationrangeof4.97to47.6μmolL − 1withalimitofdetectionof0.479μmolL − 1.Thedevelopedelectrochemicalmethodwassuccessfullyappliedforthedeterminationofosartaninpharmaceuticalformulationsamples, withresultsconsistentwiththoseobtainedbyacomparativeUV − Visspectrophotometricmethodat95%confidencelevel.Inaddition, losartanquantificationwasalsoachievedatsyntheticbiologicalfluidsamples.","author":[{"dropping − particle":"","family":"Silva","given":"TiagoAlmeida","non − dropping − particle":"","parse − names":false,"suffix":""},{"dropping − particle":"","family":"Fatibello − Filho","given":"Orlando","non − dropping − particle":"","parse − names":false,"suffix":""}],"container − title":"JournalofSolidStateElectrochemistry","id":"ITEM − 1","issue":"8","issued":{"date − parts":[["2020"]]},"page":"1827 − 1834","publisher":"JournalofSolidStateElectrochemistry","title":"Carbonblack − chitosanfilm − basedelectrochemicalsensorforlosartan","type":"article − journal","volume":"24"},"uris":["http://www.mendeley.com/documents/?uuid = 15270490 − c158 − 46aa − 82f2 − 86a7fcb6f68b"]}],"mendeley":{"formattedCitation":"[27]","plainTextFormattedCitation":"[27]","previouslyFormattedCitation":"[27]"},"properties":{"noteIndex":0},"schema":"https://github.com/citation − style − language/schema/raw/master/csl − citation.json"}[27]

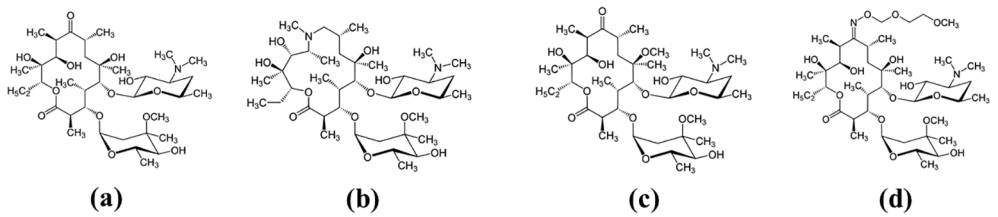

Fig. 1. Chemical structure of the macrolides erythromycin (a), azithromycin (b), clarithromycin (c), and roxithromycin (d).

where E_p is the peak potential, $E_{p/2}$ is the half-wave potential, and α is the electron transfer coefficient (α = 0.5 for irreversible processes).

The determination of each antibiotic in water and drug samples was performed by constructing a calibration curve through injections of standard solutions (10.0–160.0 μmol L^{-1}), followed by injection of sample solutions (s). Injections of sample solutions enriched with standards of the respective antibiotics (r_1 and r_2) were performed, and an additional calibration curve was constructed in the inverse direction of concentration (160.0–10.0 μmol L^{-1}).

3. Results and discussion

3.1. Morphological and electrochemical characterization of the material

SPCB is neglected in publications for GCEs modification in sensing applications, which is intriguing once different CB types are well-known as excellent materials for electrode improvement due to their nano-dimension [25]. Therefore, we decide to study such material as this can be part of a valuable field to explore. Usually, a binder agent must be chosen for the GCE modification to guarantee adhesion; for our proposes, we chose CT due to previous literature on CB application in the sensing field [27]. Also, initial assessments of the GCE modification with SPCB without CT proved to be insufficient to maintain the material over the electrode surface.

FEG-SEM analyses were conducted on the SPCB before and after the CT modification, as shown in Fig. 2a,b. One can notice that the nanometric amorphous carbon particles observed in the bare SPCB (Fig. 2a) are evidenced in the chitosan-modified sample (Fig. 2b). Due to the aggregated structures detected in both materials, a size-distribution histogram construction can be unreliable; however, carbon particle sizes between 40 and 100 nm were observed in both samples. With branched chains that create space in the aggregates, such a highly complex CB structure is easier to disperse, presents high viscosity and low wettability, which are essential properties for ink production for electrode modifications [32]. Although both materials showed such features, the CT modification improved GCE adherence with the SPCB-CT particles due to amino groups' existence on the CT molecule [33].

Raman analyses were used to investigate the SPCB samples' defectiveness before use and, consequently, the CT modification's effect on the SPCB particles' structure (Fig. 2c). The bare and modified SPCB samples presented two main vibrational signals around 1580 and 1350 cm^{-1}. The band with the lower energy is attributed to the E_{2g} mode of in-plane vibration of carbon–carbon bonds of graphite (G band), while the higher energy band corresponds (D band) to 6-membered rings breathing [34]. The simultaneous redshift, intensity increasing, and broadening of the D band indicate a more disordered structure, which is the SPCB-CT material case [35]. Specifically, the relative intensities of these D and G bands, I_D/I_G, are a convenient parameter to analyze the

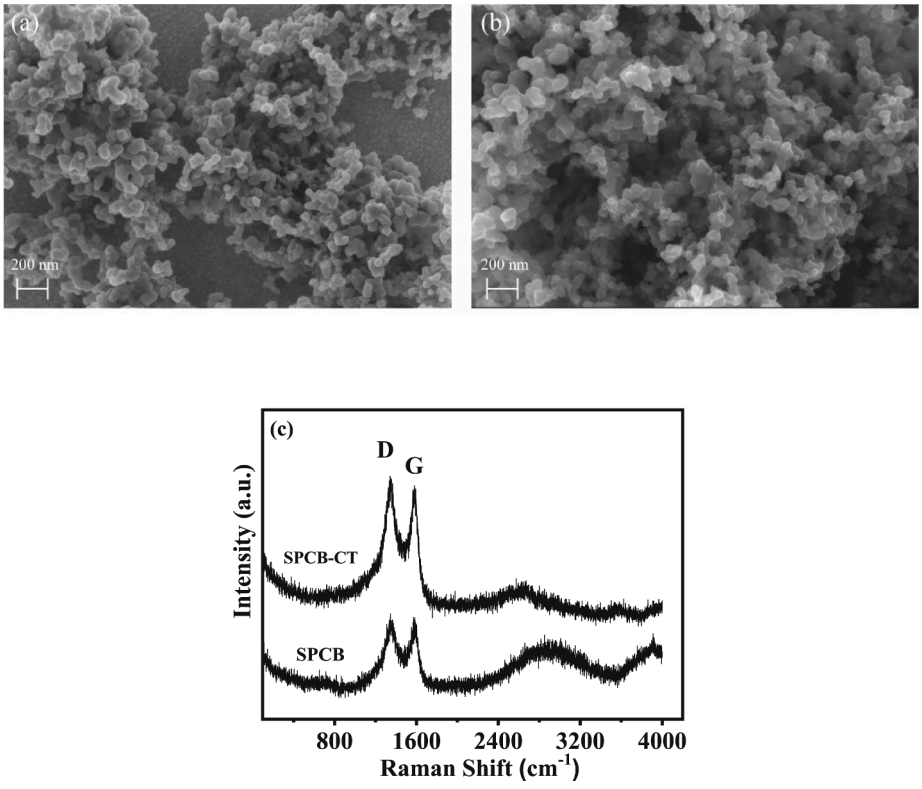

Fig. 2. SEM images of (a) SPCB, (b) SPCB-CT and (c) Raman spectra of SPCB and SPCB-CT.

level of disorder in the samples, as shown in Table S1. The nanoscale dimension of the SPCB materials is expected to present more significant defects and an increased distortion of the graphitic-like domains due to the disruption of the sp^2 systems' symmetry [36]. The $I_D/I_G = 1.6$ shows an excellent disorder for the SPCB, an interesting feature for achieving an increased capacity current. Remarkably, the chitosan-modified SPCB sample presented a ratio of 1.9. Indeed, such a result shows that the modification of the SPCB with chitosan was beneficial for the system. Also, the Raman spectra show differences in the region of higher wavelengths. The SPCB sample presents a broad peak centered at 2894.4 cm^{-1}, which suggests a convolution of peaks. The SPCB-CT sample shows a peak centered at 2632.8 cm^{-1}, attributed to the D second-order mode [37].

Once we physicochemically settled that the CT modification of SPCB particles was beneficial for the system, the electrochemical advantages should be highlighted to ensure the modification's efficiency regarding sensing properties. The electrochemical characterization of SPCB-CT/GCE was performed by CV in the presence of 1.0 *m*mol L^{-1} of the redox probe $[Fe(CN)_6]^{4-/3-}$ in 0.1 mol L^{-1} KCl. As shown in Fig. S1a, both the SPCB-CT/GCE and the bare GCE have well-defined oxidation and reduction peaks, with peak separation (ΔEp) of 60.0 *m*V and 85.0 *m*V, respectively. Also, remarkable increases in peak currents (I_p) are observed when comparing the electrodes before and after modification, which were 9.26 μA (I_{pa}) and 8.30 μA (I_{pc}) for the GCE, and 73.0 μA (I_{pa}) and 71.3 μA (I_{pc}) for the SPCB-CT/GCE, showing the electrocatalytic effect that the electrode modified with the SPCB-CT film can provide. Then, a study of the variation of the scanning rate (*v*) was carried out under the same conditions, where the values of I_{pa} were monitored as a function of the scan rate (*v*). In Fig. S1b, one can observe the linear response between I_{pa} and $v^{1/2}$ (r = 0.997) indicates a diffusional-controlled process ruled by the Randles–Ševćik equation [31]. Based on this equation, the electroactive area of the SPCB-CT/GCE obtained was 1.38 cm^2. Such a result represents a 20-fold increase over the GCE's area, which was 0.07 cm^2.

The EIS is a powerful tool to investigate surface phenomena and changes in material bulk properties, suitable for a direct comparison between the GCE and SPCB- CT/GCE materials. The measurements were carried out in 5.0 *m*mol L^{-1} of the redox pair $[Fe(CN)_6]^{4-/3-}$ in 0.1 mol L^{-1} of KCl. Fig. S2 displays the impedance spectra obtained for the electrodes. The bare GCE shows the characteristic Nyquist-plot format, with a single semicircle associated with the charge transfer process in the high-frequency region and a linear region attributed to diffusion control in the lower frequency region.[38] By comparison, the GCE modification with SPCB-CT also presented a semicircle and linear region; however, the GCE arc radii is considerably larger than the observed for SPCB-CT/GCE, implying lower electron-transfer resistance kinetics of the redox probe for the modified electrode. The solution resistance was quite different for the electrodes, i.e., 121.0 and 12.6 Ω for GCE and SPCB-CT/GCE, respectively; the latter is considerably reduced, indicating faster electron transfer processes in the modified electrode. The excellent properties shown herein present the material as an attractive alternative in the preparation of electrochemical sensors, as well as other types of CB that are already used for this purpose, e.g., Vulcan XC72R, N220, and M 1100 [39–41].

3.2. Voltammetric behavior of ERY

The electrochemical response of ERY was initially investigated by CV; measurements were performed in the absence and presence of 40.0 μmol L^{-1} ERY in 0.1 mol L^{-1} BR buffer (pH 7.0) as supporting electrolyte. For comparison purposes, the electrochemical response of the antibiotic was evaluated using the bare GCE and the SPCB-CT/GCE as working electrodes. Fig. 3 presents the cyclic voltammograms obtained over a potential range from + 0.45 V to + 1.10 V *vs*. Ag/AgCl, $KCl_{(sat.)}$. In both cases, scanning in the anodic potential direction presents oxidation peaks at + 0.95 V and + 0.77 V for GCE and SPCB-CT/GCE, respectively. At the reversing scanning, no peaks of reduction in the potential range used are apparent, suggesting that ERY undergoes an irreversible oxidation process under these conditions. Furthermore, the anodic peak current value obtained for the SPCB-CT/GCE was considerably higher than that verified using the bare electrode. Thus, a 12-fold increase in current and a potential anticipation of 180.0 *m*V were obtained when comparing the E_p obtained for the GCE with the SPCB-CT/GCE.

3.2.1. Effect of pH and scan rate

The supporting electrolyte's pH effect (from 4.0 to 10.0) was evaluated through the signals obtained by recording linear scanning voltammograms in the anodic direction in the presence of 40.0 μmol L^{-1} ERY in 0.1 μmol L^{-1} BR buffer (Fig. S3). Fig. S3a presents the oxidation peaks at the chosen pH range, while Fig. S3b allows us numerical analyses. An increase in I_p values up to pH 7.0 is noted, and after that, a gradual decrease of the signal is observable with pH augmentation. Furthermore, a linear dependence of the peak potential (E_p) to less positive values (Fig. S3b) causes a displacement rate of –60 *m*V per pH unit (r = 0.998). This value suggests that the number of protons involved in the ERY oxidation mechanism equals the number of electrons [42]. Using the voltammogram for oxidation of ERY at pH 7.0 (Fig. S3a), the value of E_p–$E_{p/2}$ was 45.0 *m*V and, for irreversible processes, [50] *n* was estimated as two. Therefore, two protons and two electrons are involved in the oxidation of ERY on the surface of SPCB-CT/GCE. According to the literature, oxidation occurs at the tertiary amino group moiety of one of the sugars of ERY molecule. [43]. The effect of scan rate (*v*) on ERY oxidation was evaluated in a range between 5.0 and 300.0 *m*V s^{-1} (Fig. S4a). One can notice that the increase in scan rate causes an increase in I_p and a shift in E_p towards more positive potentials, which is a consequence of the irreversibility of the ERY oxidation [42]. Furthermore, a linear relationship was verified between I_p and *v* (r = 0.999) and between log I_p and log *v*, with a slope of 0.957 (Fig. S4b,c), indicating that the oxidation of ERY in SPCB-CT/GCE is an adsorption-controlled process [43].

3.2.2. Effect of supporting electrolyte composition

The effect of different chemical compositions of the supporting electrolyte was also evaluated at pH 7.0. The following solutions were tested at a concentration of 0.1 mol L^{-1} each: BR, Sörensen, McIlvaine buffers, and KCl solution. The antibiotic behaves similarly to the previously shown, with an irreversible oxidation peak for all the electrolytes. However, differences in intensity and peak definition were observed, in which the 0.1 mol L^{-1} Sörensen buffer presented stronger signal intensity, definition, and stability. Thus, to obtain the best experimental conditions for developing the method, a new pH study within the buffering range (6.2–7.8) and a study of the supporting electrolyte concentration were carried out. The pH study in the 0.1 mol L^{-1} Sörensen buffer solution, shown in Fig. S5a, demonstrated a slight variation in Ip values and a shift of E_p to less positive values with increasing pH. Therefore, pH 7.8 was chosen as the optimum condition once the reaction occurs at less positive potentials. The effect of the concentration of the supporting electrolyte (Fig. S5b) demonstrated that, in the concentration range studied, 0.5 mol L^{-1} presented higher current intensity and lower standard deviation, being the chose concentration for other studies.

3.3. Determination of macrolide antibiotics

According to mechanisms presented in the literature, the first step of the process is the removal of an electron from the nitrogen atom to form an aminium cation radical. This reaction product undergoes demethylation, resulting in the corresponding secondary amine [44]. The exact mechanism is attributed to the oxidation of its ERI's derivatives AZY, CLA, and ROX [45–47]. Similar behavior was also observed when recording the voltammetric profile of these four antibiotics on the surface of SPCB-CT/GCE. Fig. S6 shows the cyclic voltammograms of ERY,

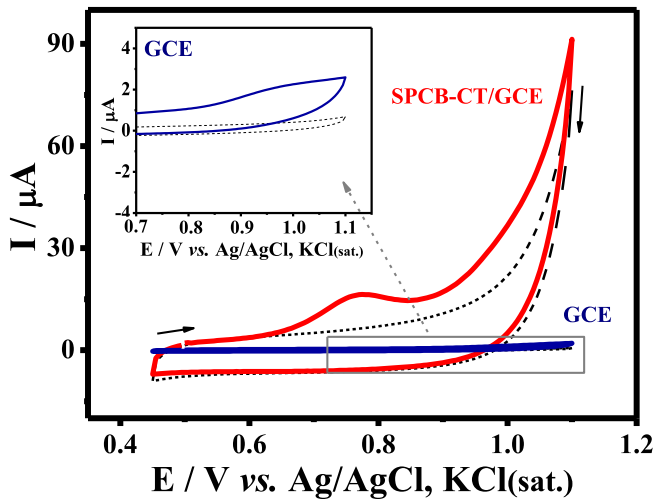

Fig. 3. Cyclic voltammograms of the bare electrode (GCE) and modified with Super P carbon black (SPCB-CT/GCE) in 0.1 mol L^{-1} buffer BR (pH 7.0) in the absence (dotted lines) and in the presence (solid lines) of ERY (40 μmol L^{-1}). Insert: Voltamograms obtained with GCE. $\nu = 50$ mV s^{-1}; step potential = 5 *m*V.

AZI, CLA, and ROX under the experimental conditions optimized in the previous item. As illustrated in the figure, the macrolide antibiotics AZI, CLA, and ROX showed their respective oxidation peaks in positions and intensities similar to ERY. This effect can be explained by the fact that these four antibiotics follow the exact oxidation mechanism. Based on this, it was decided to verify the method's applicability in determining any of these four antibiotics.

3.3.1. Hydrodynamic voltammograms

Hydrodynamic voltammograms were constructed in the BIA system for each antibiotic in the potential range of 0.0 to 1.1 V *vs.* PRE to verify the analytical signal and define the oxidation potential. Therefore, 50.0 μmol L^{-1} solutions of each antibiotic were injected in triplicate directly onto the surface of the SPCB-CT/SPE, applying fixed potentials (interval potential of 0.05 V). The resulting hydrodynamic voltammograms are shown in Fig. S7, and each point represents the average ($n = 3$) obtained as a function of the respective potentials applied for each amperometric measurement.

The oxidation processes of the four antibiotics studied under hydrodynamic conditions started at potentials around +0.4 V *vs.* PRE. After that, the current values increase with the increase of the applied potential. The parameters for choosing the potentials for the subsequent amperometric measurements were based on the highest current values with the lowest standard deviation from the mean. The selected potentials were: +0.85 for ERY and ROX, and +0.90 for AZI and CLA.

3.3.2. Optmization of the BIA-AMP paramters

Some parameters related to the BIA-AMP system were optimized to obtain higher current values, namely, injection volume (V_{inj}) and dispensing rate (R_{dis}). The experiments were carried out by injecting 50.0 μmol L^{-1} ERY solutions ($n = 3$) using an electronic micropipette that allows injection volume variations from 10.0 to 200.0 μL and dispensing rate from 18.9 to 100.0 μL s^{-1}. The results presented in Fig. S8a show that the values of I_p increase as the injected volume increases. However, volumes above 100 μL generate higher standard deviation values, compromising the method's precision. Then, a volume of 100 μL was chosen for the following measurements. The results obtained for the R_{dis} (Fig. S8b) show that, at 100 μL s^{-1}, higher current values are obtained (keeping the injection volume at 100 μL). This effect occurs due to decreased analyte dispersion in the sample zone over the SPCB-CT/SPE at higher velocities. Therefore, this was the chosen dispensing speed for the other experiments.

3.3.3. Application of the BIA-AMP method

After optimizing the parameters of the BIA-AMP system, a repeatability study was carried out to assess the method's precision. Thus, a sequence of 25 injections (50.0 μmol L^{-1} ERY solution each) was performed on the SPCB-CT/SPE surface in a BIA-AMP system, using the previously optimized parameters. Fig. 4a shows no significant variation in I_p values over the 25 injections (RSD = 0.98%), evidencing the precision of the proposed method. In addition, the analytical frequency (AF) was estimated at 125 injections h^{-1}, which is highly superior to the AF of other methods used to determine macrolides [48,49].

Subsequently, the reproducibility of the SPCB-CT/SPE was evaluated. At this stage, analyzes were performed successively for ten consecutive days. For each daily measurement, SPCB-CT/SPE was prepared before each analysis using just a new SPE. Consecutive injections of 100 μmol L^{-1} ERY were performed using the parameters optimized for the BIA-AMP system. The results obtained (Fig. 4b) show the excellent repeatability of the method, considering the eight consecutive days of analysis (RSD = 2.60 %). Furthermore, the modification of the commercial SPE ensured the reuse of this substrate for eight successive days of study, reducing the cost of the method (the modifier was removed daily after the analysis without compromising the integrity of the SPE).

The dependence of the analytical signal on concentration was evaluated for ERY, AZI, CLA, and ROX in 0.5 mol L^{-1} Sörensen buffer (pH 7.0) as supporting electrolyte. Injections ($n = 3$) of standard solutions in the concentration range of 1.0–190.0 μmol L^{-1} for ERY, AZI, CLA, and ROX were performed. The BIA amperograms and their respective calibration curves (Fig. S9) were recorded in ascending and descending order of concentration. The results show the linear behavior in the wide range studied for the four antibiotics. From these data, it was possible to estimate the LOD and LOQ values. These results are shown in Table 1.

Subsequently, the proposed method was applied to determine the four antibiotics (individually) in groundwater samples. Fig. 5 shows the amperograms obtained by triplicate injections of five solutions in increasing concentrations of ERY (i), AZI (iii), CLA (v), and ROX (vii) (a–e: 10.0–160.0 μmol L^{-1}), water sample (s), samples enriched with two known concentrations of the respective compounds (r_1 and r_2), and finally standard solutions in decreasing order of concentration (e–a: 160.0–10.0 μmol L^{-1}). The results obtained in this step confirmed the linear behavior of the system ($r \geq 0.998$) and sensitivity values close to the values obtained in the previous test for the respective antibiotics, showing the excellent reproducibility of the method. The signals acquired for the water samples did not detect the antibiotics, or they are present at concentrations below the LOD of the method. The recovery values obtained for the enriched water samples range between 96.0% and 104.7%, evidencing the good accuracy of the proposed method. Some sample analyses presented negative signals; however, it is straightforwardly explainable. A similar effect, the so-called Schlieren effect [50], is common in flow injection analysis measurements with spectrophotometry detection. This effect is always concentration-dependent and temperature-dependent; it occurs when a sample solution, which is different from the carrier solution, is injected into the system. The difference in the refraction index between the sample and the carrier will affect the analytical signal, causing some negative transient signals. Similarly, when a solution is inserted into the BIA cell with electrochemical detection, solutions with different ionic strengths will affect varying extensions on the double layer interface. As the sample preparation is just a dilution process, we suppose that the effect observed for the "negative" sample signal is due to the difference in the ionic strength between the sample and the supporting electrolyte into the BIA cell. The same effect can be observed in the method developed by De Faria et al. to determine sulfanilamide by batch injection analysis using a reduced graphene oxide electrode [51]. In addition, the observed effect did not compromise the analytical signal of the antibiotics or the performance of the proposed BIA system (Table 2).

Drug samples containing AZI and CLA as active ingredients were analyzed to investigate the sensor's feasibility in quantifying these

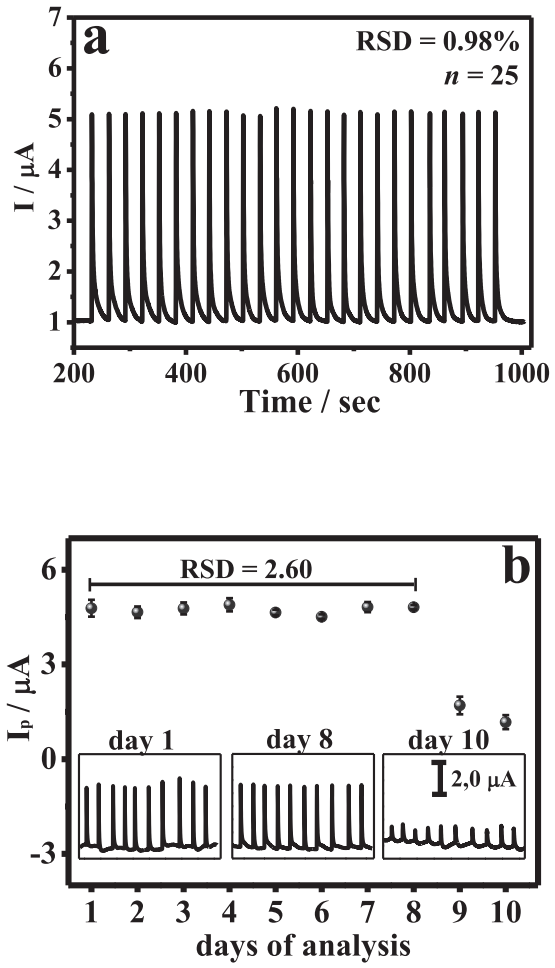

Fig. 4. **(a)** Amperogram obtained from successive injections of ERY 50.0 µmol L^{-1} ($n = 25$) into the BIA-AMP system. **(b)** Reproducibility study for SPCB-CT/SPE was obtained through the average of ten injections of 100.0 µmol L^{-1} ERY solution over ten days. E = +0.85 V; Supporting electrolyte: 0.5 mol L^{-1} Sörensen buffer (pH 7.8); $V_{inj} = 100$ µL; $R_{dis} = 100$ µL s^{-1}. Insert: Amperograms obtained on the 1st, 8th, and 10th day of analysis.

compounds in pharmaceutical formulations. Analyzes were performed similarly to the water analysis described before. The amperograms and their respective calibration curves are shown in Fig. S10. Table 3 summarizes the results of the quantification of AZI and CLA in the drugs. The mass values obtained for each of the samples analyzed were below the value described on the drug label. However, these values are within the range acceptable by the Brazilian Pharmacopoeia [52]. Also, recovery values close to 100% in all analyzed samples confirm the excellent accuracy of the method. Although recent literature has proposed some electrochemical detection of macrolide antibiotics, our system presents superior performance and is cheaper and easier to prepare. For example, Rebelo et al. designed a molecularly imprinted polymer prepared on a disposable SPE, with recoveries in the range between 84 and 123%. Their material counts on an interesting synthesis method; however, their sensor is more expensive and time-consuming for its preparation. Their reproducibility was 9.3 and 11.6% for concentrations of 2 and 8 µmol L^{-1}. Also, our linear range reached a wide range (1.0–190.0 µmol L^{-1}), while they obtained a linear relationship between 0.5 and 10.0 mmol L^{-1} [53]. Vajdle et al. obtained a silver-amalgam film electrode with linearity in concentration ranges 4.81–23.3 mg mL^{-1}, and 1.96–28.6 mg L^{-1} for AZI and CLA, which is interesting, but also presents a lower performance compared to our system [54]. Other methods were described in the literature using chromatography, which was avoided by us, due to the required equipment [55–57].

Table 1
Analytical signal dependence parameters with macrolide concentration in the presence of 0.5 mol L^{-1} Sörensen buffer (pH 7.8) in the BIA-AMP system.

	Linear range (µmol L^{-1})	Slope (µA L µmol^{-1})	Intercept (µA)	r	LOD (µmol L^{-1})	LOQ (µmol L^{-1})
ERY	1.0–190.0	0.057 ± 0.001	0.281 ± 0.010	0.999	0.191	0.637
AZI	1.0–190.0	0.072 ± 0.002	0.150 ± 0.068	0.995	0.153	0.509
CLA	10.0–190.0	0.069 ± 0.002	0.774 ± 0.212	0.998	0.161	0.536
ROX	1.0–190.0	0.062 ± 0.002	0.095 ± 0.035	0.999	0.186	0.619

Table 4 compares the proposed BIA-AMP method with other electroanalytical methods reported in the literature to determine macrolide antibiotics ERY, AZI, CLA, and ROX, highlighting the sensor used, technique, linear range, detection limit, analytical frequency, and sample. In this comparison, the BIA method proposed herein presented analytical performance superior to most methods developed to determine any of the four antibiotics. However, sensors prepared from molecularly immobilized polymers (MIP's) showed a higher linear range and lower LOD than the obtained in our studies. Considering that in the preparation processes of MIP's, large volumes of organic solvents and long preparation times are necessary, the method proposed here is superior once it is easy to prepare, with minimal consumption of organic solvent, cheap, and presents a quick analysis. In addition, the proposed BIA method is the only so far that can be applied in the determination of any of these four macrolide antibiotics.

4. Conclusions

We demonstrate the potential of using SPCB as a modifier in printed carbon electrodes to determine four macrolide antibiotics (ERI, AZI, CLA, and ROX) using the BIA-AMP system. Optimizations performed both in the modifier and in the system parameters ensured better analytical performance of the method, such as lower detection and quantification limits, wide linear range, higher analytical sensitivity, and frequency than other electroanalytical methods reported in the literature. Furthermore, it allows applying the same method, without significant changes, to determine any one of the four compounds, with the portability advantage that the BIA system presents. The procedure was successfully applied in determining the four macrolide antibiotics in an environmental and pharmaceutical sample. The results obtained demonstrated the accuracy of the proposed method, having attractive characteristics for its application in routine analyses.

CRediT authorship contribution statement

William Barros Veloso: Data curation, Formal analysis, Investigation, Validation, Visualization, Writing – original draft. **Anny Thalia de Freitas Oliveira Almeida:** Data curation, Formal analysis, Validation. **Lara Kelly Ribeiro:** Data curation, Formal analysis. **Marcelo de Assis:** Data curation, Formal analysis. **Elson Longo:** Visualization, Writing – review & editing. **Marco Aurélio Suller Garcia:** Data curation, Visualization, Writing – review & editing. **Auro Atsushi Tanaka:** Visualization, Writing – original draft. **Iranaldo Santos da Silva:** Conceptualization, Visualization, Writing – original draft, Writing – review & editing. **Luiza Maria Ferreira Dantas:** Project administration, Resources, Visualization, Writing – original draft, Writing – review & editing.

Declaration of Competing Interest

The authors declare that they have no known competing financial

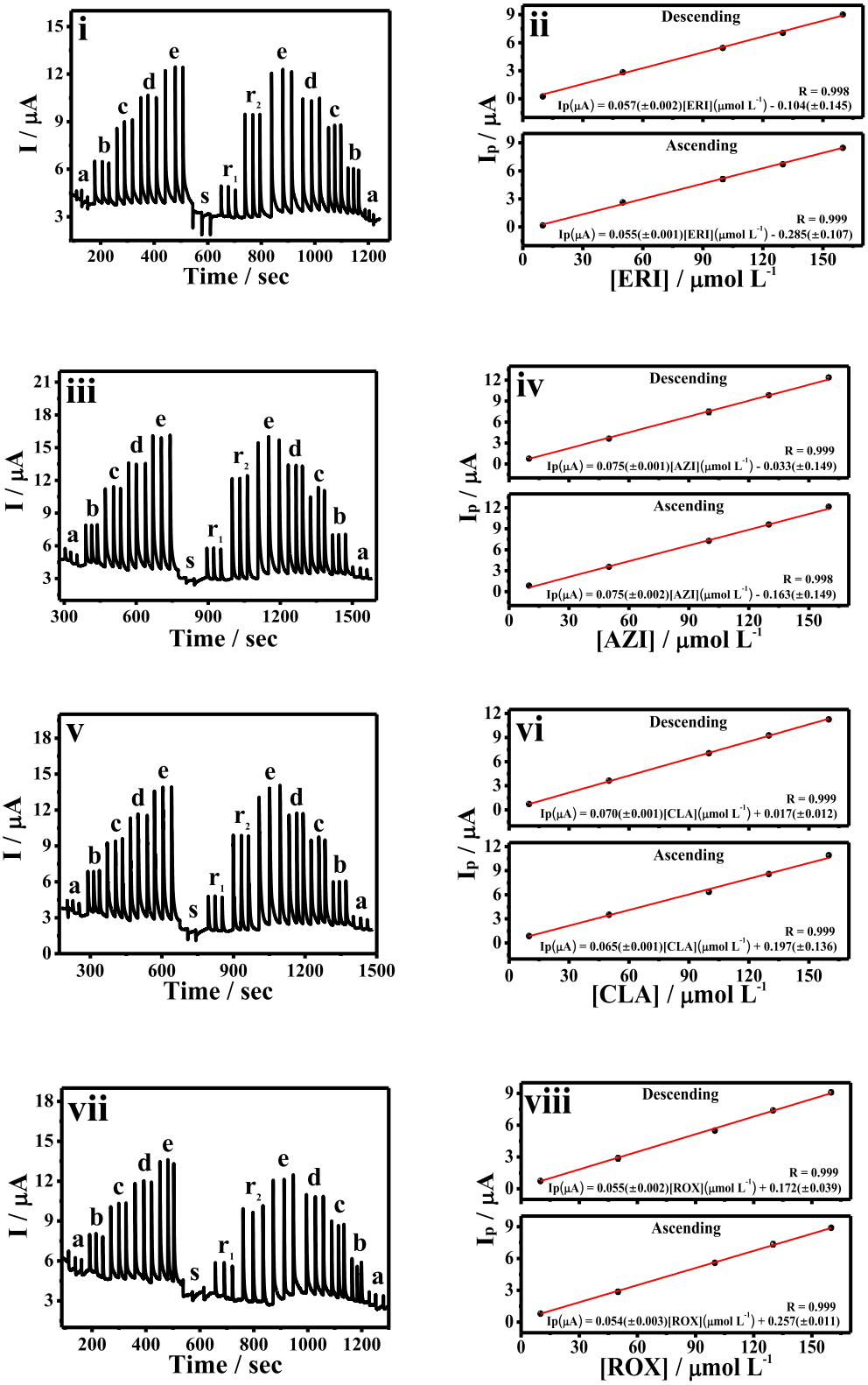

Fig. 5. Amperogram obtained through injections (n = 3) in a BIA-AMP system of standard solutions of ERY (i), AZI (iii), CLA (v), and ROX (vii) at different concentrations (a–e: 10–160 µmol L^{-1}), water sample (s) and sample enriched in two concentrations of the respective standards (r_1 and r_2). Supporting electrolyte: 0.5 mol L^{-1} Sörensen buffer (pH 7.8); V_{inj} = 100 µL; R_{dis} = 100 µL s^{-1}. Calibration curves were obtained from the values of I_p in the increasing and decreasing directions of concentration of ERY (ii), AZI (iv), CLA (vi), and ROX (viii).

Table 2
ERY, AZI, CLA, and ROX concentration in pond water samples by the proposed BIA-AMP method and added and recovery values.

		Added (μmol L^{-1})	Found (μmol L^{-1})	Recovery (%)
ERY	s	0	<LOD	–
	r_1	40.0	38.4 ± 1.5	96.0 ± 3.8
	r_2	120.0	122.8 ± 0.7	102.3 ± 0.6
AZI	s	0	<LOD	–
	r_1	40.0	39.2 ± 1.3	98.1 ± 3.4
	r_2	120.0	125.6 ± 2.0	104.7 ± 1.7
CLA	s	0	<LOD	–
	r_1	40.0	39.5 ± 1.6	98.8 ± 4.1
	r_2	120.0	117.4 ± 1.7	97.8 ± 1.3
ROX	s	0	<LOD	–
	r_1	40.0	39.6 ± 1.2	99.9 ± 3.0
	r_2	120.0	123.2 ± 4.7	102.6 ± 3.9

Table 3
Determination of AZI and CLA in pharmaceutical samples and recovery testing.

	Mass (g/capsule)	Recovery test				
AZI	s_1	0.484 ± 0.04		Added (μmol L^{-1})	Found (μmol L^{-1})	Recovery (%)
	s_2	0.478 ± 0.01	$\mathbf{r_1}$	30	29.9 ± 0.9	99.6 ± 3.0
	s_3	0.491 ± 0.01	$\mathbf{r_2}$	100	95.6 ± 1.8	95.6 ± 1.8
CLA	s_1	0.487 ± 0.05		**Added (μmol L^{-1})**	**Found (μmol L^{-1})**	**Recovery (%)**
	s_2	0.488 ± 0.02	$\mathbf{r_1}$	30	31.5 ± 3.4	105.1 ± 9.4
	s_3	0.479 ± 0.01	$\mathbf{r_2}$	100	100.8 ± 2.3	100.8 ± 2.3

Table 4
Comparison of the analytical parameters of the proposed system with other methods for determining macrolide antibiotics.

Macrolide	Technique	Detection	Linear range (μmol L^{-1})	LOD (μmol L^{-1})	AF (Injections h^{-1})	Sample (s)	Ref.
AZI	SWV	Hg(Ag)FE	6.42–31.1	1.92	n.m.	Drug	[54]
CLA			2.62–38.2	0.79			
ROX			1.77–30.9	0.53			
ERY	FIA	SDS/SPCE	1.36–34.1	0.19	n.m.	Environmental (water)	[6]
ERY	SWV	Hg(Ag)FE	6.17–40.6	1.85	n.m	Drug and urine	[58]
ERY	SWV	BDD	6.8–81.1	1.1	n.m.	Environmental (water)	[59]
AZI	FIA	UV–Vis λ = 540 nm	66.7–2.14 × 10^3	8.81	65	Drug	[60]
AZI	DPV	MIP	0.5–10.0	0.08	n.m	Environmental (water)	[53]
CLA	Potentiometry	MIP	1.0–5000.0	0.8	240	Drug	[61]
ROX	Coulometry	SWNT/GC	5.0–100.0	0.5	n.m	Drug	[62]
AZI	FIA	UV–Vis λ = 525 nm	5.34–26.7	3.94	60	Drug	[63]
ERY	AMP	SPCB-CT/GCE	1.0–190.0	0.19	125	Environmental (water) and drugs	This work
AZI			1.0–190.0	0.15			
CLA			10.0–190.0	0.16			
ROX			1.0–190.0	0.18			

SWV–Square Wave Voltammetry; Hg(Ag)FE–Silver amalgam film electrode; BDD–Boron Doped Diamond; FIA–Flow Injection Analysis; SDS/SPCE–Screen-printed carbon electrode modified with sodium dodecyl sulfate modified; MIP–Molecularly Imprinted Polymer; SWNT/GC–Glassy carbon electrode modified with single-walled carbon nanotubes; UV–Vis–Ultraviolet and visible spectrophotometry; AMP–amperometry. PDV–Differential Pulse Voltammetry; n.m–not mentioned.

interests or personal relationships that could have appeared to influence the work reported in this paper.

Acknowledgments

The authors are grateful to funding agencies: CNPq fellow-Brazil (grant no. 205220/2018-5, 133321/2019-3), CNPq/INCTBioanalítica (Project 465389/2014-7), CAPES (Project SCBA 88887.472618/2019-00), and FAPEMA (Project UNIVERSAL-01372/17).

Appendix A. Supplementary data

Supplementary data to this article can be found online at https://doi.org/10.1016/j.microc.2021.106939.

References

[1] I. Senta, S. Terzic, M. Ahel, Analysis and occurrence of macrolide residues in stream sediments and underlying alluvial aquifer downstream from a pharmaceutical plant, Environ. Pollut. 273 (2021) 116433, https://doi.org/10.1016/j.envpol.2021.116433.
[2] C. Hu, Y. Zhang, Y.u. Zhou, Z.-F. Liu, Q. Meng, X.-S. Feng, A review of pretreatment and analysis of macrolides in food (Update Since 2010), J. Chromatogr. A. 1634 (2020) 461662, https://doi.org/10.1016/j.chroma.2020.461662.
[3] A. Mahmoudi, R.-E.-A. Fourar, M.S. Boukhechem, S. Zarkout, Microbiological assay for the analysis of certain macrolides in pharmaceutical dosage forms, Int. J. Pharm. 491 (1-2) (2015) 285–291, https://doi.org/10.1016/j.ijpharm.2015.06.027.
[4] J. Wang, Z. Yang, X. Wang, N. Yang, Capillary electrophoresis with gold nanoparticles enhanced electrochemiluminescence for the detection of roxithromycin, Talanta 76 (1) (2008) 85–90, https://doi.org/10.1016/j.talanta.2008.02.006.

[5] R.A. Pérez, B. Albero, M. Férriz, J.L. Tadeo, Analysis of macrolide antibiotics in water by magnetic solid-phase extraction and liquid chromatography–tandem mass spectrometry, J. Pharm. Biomed. Anal. 146 (2017) 79–85, https://doi.org/10.1016/j.jpba.2017.08.013.

[6] A. Veseli, F. Mullallari, F. Balidemaj, L. Berisha, Ľ. Švorc, T. Arbneshi, Electrochemical determination of erythromycin in drinking water resources by surface modified screen-printed carbon electrodes, Microchem. J. 148 (2019) 412–418, https://doi.org/10.1016/j.microc.2019.04.086.

[7] A. Hossain, S. Nakamichi, M. Habibullah-Al-Mamun, K. Tani, S. Masunaga, H. Matsuda, Occurrence and ecological risk of pharmaceuticals in river surface water of Bangladesh, Environ. Res. 165 (2018) 258–266, https://doi.org/10.1016/j.envres.2018.04.030.

[8] W. Li, Y. Shi, L. Gao, J. Liu, Y. Cai, Occurrence of antibiotics in water, sediments, aquatic plants, and animals from Baiyangdian Lake in North China, Chemosphere 89 (11) (2012) 1307–1315, https://doi.org/10.1016/j.chemosphere.2012.05.079.

[9] European Commission, Development of the first Watch List under the Environmental Quality Standards Directive water policy, 2015. https://doi.org/10.2788/101376.

[10] S. Bhimani, G. Sanghvi, T. Pethani, G. Dave, V. Airao, T. Sharma, N. Sheth, D. Vaishnav, Development of the UV spectrophotometric method of azithromycin in API and stress degradation studies, Int. Lett. Chem. Phys. Astron. 68 (2016) 48–53. https://doi.org/10.18052/www.scipress.com/ilcpa.68.48.

[11] P.T. Thanh Ha, A. Van Schepdael, E. Roets, J. Hoogmartens, Investigating the potential of erythromycin and derivatives as chiral selector in capillary electrophoresis, J. Pharm. Biomed. Anal. 34 (5) (2004) 861–870, https://doi.org/10.1016/j.jpba.2003.11.004.

[12] B. Shao, D. Chen, J. Zhang, Y. Wu, C. Sun, Determination of 76 pharmaceutical drugs by liquid chromatography-tandem mass spectrometry in slaughterhouse wastewater, J. Chromatogr. A. 1216 (47) (2009) 8312–8318, https://doi.org/10.1016/j.chroma.2009.08.038.

[13] S.-C. Kim, K. Carlson, Quantification of human and veterinary antibiotics in water and sediment using SPE/LC/MS/MS, Anal. Bioanal. Chem. 387 (4) (2007) 1301–1315, https://doi.org/10.1007/s00216-006-0613-0.

[14] G.A.C. Ribeiro, C.Q. da Rocha, W.B. Veloso, L.M.F. Dantas, E.M. Richter, I.S. da Silva, A.A. Tanaka, Flow-through amperometric methods for detection of the bioactive compound quercetin: performance of glassy carbon and screen-printed carbon electrodes, J. Solid State Electrochem. 24 (8) (2020) 1759–1768, https://doi.org/10.1007/s10008-020-04599-x.

[15] E.F. Silva, A.A. Tanaka, R.N. Fernandes, R.A.A. Munoz, I.S. da Silva, Batch injection analysis with electrochemical detection for the simultaneous determination of the diuretics furosemide and hydrochlorothiazide in synthetic urine and pharmaceutical samples, Microchem. J. 157 (2020) 105027, https://doi.org/10.1016/j.microc.2020.105027.

[16] D.T. Gimenes, M.C. Marra, J.M. de Freitas, R.A. Abarza Muñoz, E.M. Richter, Simultaneous determination of captopril and hydrochlorothiazide on boron-doped diamond electrode by batch injection analysis with multiple pulse amperometric detection, Sens. Actuators, B Chem. 212 (2015) 411–418, https://doi.org/10.1016/j.snb.2015.01.132.

[17] W.B. Veloso, G.A.C. Ribeiro, C.Q. da Rocha, A.A. Tanaka, I.S. da Silva, L.M. F. Dantas, Flow-through amperometric determination of ampicillin using a copper electrode in a batch injection analysis system, Measurement 155 (2020) 107516, https://doi.org/10.1016/j.measurement.2020.107516.

[18] M. Li, Y.T. Li, D.W. Li, Y.T. Long, Recent developments and applications of screen-printed electrodes in environmental assays-A review, Anal. Chim. Acta. 734 (2012) 31–44, https://doi.org/10.1016/j.aca.2012.05.018.

[19] K. Ghanbari, M. Roushani, A novel electrochemical aptasensor for highly sensitive and quantitative detection of the streptomycin antibiotic, Bioelectrochemistry 120 (2018) 43–48, https://doi.org/10.1016/j.bioelechem.2017.11.006.

[20] M. Yadav, V. Ganesan, R. Gupta, D.K. Yadav, P.K. Sonkar, Cobalt oxide nanocrystals anchored on graphene sheets for electrochemical determination of chloramphenicol, Microchem. J. 146 (2019) 881–887, https://doi.org/10.1016/j.microc.2019.02.025.

[21] H. Wang, H. Zhao, X. Quan, S. Chen, Electrochemical determination of tetracycline using molecularly imprinted polymer modified carbon nanotube-gold nanoparticles electrode, Electroanalysis 23 (8) (2011) 1863–1869, https://doi.org/10.1002/elan.201100049.

[22] A. Munawar, M.A. Tahir, A. Shaheen, P.A. Lieberzeit, W.S. Khan, S.Z. Bajwa, Investigating nanohybrid material based on 3D CNTs@Cu nanoparticle composite and imprinted polymer for highly selective detection of chloramphenicol, J. Hazard. Mater. 342 (2018) 96–106, https://doi.org/10.1016/j.jhazmat.2017.08.014.

[23] P.B. Deroco, R.C. Rocha-Filho, O. Fatibello-Filho, A new and simple method for the simultaneous determination of amoxicillin and nimesulide using carbon black within a dihexadecylphosphate film as electrochemical sensor, Talanta 179 (2018) 115–123, https://doi.org/10.1016/j.talanta.2017.10.048.

[24] F.C. Vicentini, A.E. Ravanini, L.C.S. Figueiredo-Filho, J. Iniesta, C.E. Banks, O. Fatibello-Filho, Imparting improvements in electrochemical sensors: evaluation of different carbon blacks that give rise to significant improvement in the performance of electroanalytical sensing platforms, Electrochim. Acta 157 (2015) 125–133, https://doi.org/10.1016/j.electacta.2014.11.204.

[25] V. Mazzaracchio, M.R. Tomei, I. Cacciotti, A. Chiodoni, C. Novara, M. Castellino, G. Scordo, A. Amine, D. Moscone, F. Arduini, Inside the different types of carbon black as nanomodifiers for screen-printed electrodes, Electrochim. Acta 317 (2019) 673–683, https://doi.org/10.1016/j.electacta.2019.05.117.

[26] M. Youssry, L. Madec, P. Soudan, M. Cerbelaud, D. Guyomard, B. Lestriez, Non-aqueous carbon black suspensions for lithium-based redox flow batteries: rheology and simultaneous rheo-electrical behavior, Phys. Chem. Chem. Phys. 15 (2013) 14476–14486, https://doi.org/10.1039/c3cp51371h.

[27] L.P. Silva, T.A. Silva, F.C. Moraes, O. Fatibello-Filho, Carbon black-chitosan film-based electrochemical sensor for losartan, J. Solid State Electrochem. 24 (8) (2020) 1827–1834, https://doi.org/10.1007/s10008-020-04541-1.

[28] T. Morita, R.M.V. Assumpção, Manual de soluções, reagentes e solventes: padronização, preparação e purificação, São Paulo -, Brasil, 1972.

[29] R.M. Cardoso, D.M.H. Mendonça, W.P. Silva, M.N.T. Silva, E. Nossol, R.A.B. da Silva, E.M. Richter, R.A.A. Muñoz, 3D printing for electroanalysis: from multiuse electrochemical cells to sensors, Anal. Chim. Acta. 1033 (2018) 49–57, https://doi.org/10.1016/j.aca.2018.06.021.

[30] Analytical Methods Committee, Recommendations for the definition, estimation and use of the detection limit, Analyst 112 (1987) 199–204, https://doi.org/10.1039/AN9871200199.

[31] S.J. Konopka, B. McDuffie, Diffusion coefficients of ferri- and ferrocyanide ions in aqueous media, using twin-electrode thin-layer electrochemistry, Anal. Chem. 42 (14) (1970) 1741–1746, https://doi.org/10.1021/ac50160a042.

[32] D. Pantea, H. Darmstadt, S. Kaliaguine, C. Roy, Electrical conductivity of conductive carbon blacks: influence of surface chemistry and topology, Appl. Surf. Sci. 217 (1-4) (2003) 181–193, https://doi.org/10.1016/S0169-4332(03)00550-6.

[33] E.B. Aydın, M. Aydın, M.K. Sezgintürk, Electrochemical immunosensor based on chitosan/conductive carbon black composite modified disposable ITO electrode: an analytical platform for p53 detection, Biosens. Bioelectron. 121 (2018) 80–89, https://doi.org/10.1016/j.bios.2018.09.008.

[34] C.B. Aquino, D.A. Nagaoka, M.M. Machado, E.G. Cândido, A.G.M. da Silva, P.H. C. Camargo, S.H. Domingues, Chemical versus electrochemical: what is the best synthesis method to ternary GO/WO3NW/PAni nanocomposites to improve performance as supercapacitor? Electrochim. Acta 356 (2020) 136786, https://doi.org/10.1016/j.electacta.2020.136786.

[35] D.P. Upare, S. Yoon, C.W. Lee, Nano-structured porous carbon materials for catalysis and energy storage, Korean J. Chem. Eng. 28 (3) (2011) 731–743, https://doi.org/10.1007/s11814-010-0460-8.

[36] A. Coccato, J. Jehlicka, L. Moens, P. Vandenabeele, Raman spectroscopy for the investigation of carbon-based black pigments, J. Raman Spectrosc. 46 (2015) 1003–1015, https://doi.org/10.1002/jrs.4715.

[37] H.J. Seong, A.L. Boehman, Evaluation of Raman parameters using visible Raman microscopy for soot oxidative reactivity, Energy Fuels 27 (3) (2013) 1613–1624, https://doi.org/10.1021/ef301520y.

[38] Y. Wei, L. Luo, Y. Ding, X. Liu, Y. Chu, A glassy carbon electrode modified with poly(eriochrome black T) for sensitive determination of adenine and guanine, Microchim. Acta 180 (9-10) (2013) 887–893, https://doi.org/10.1007/s00604-013-1007-6.

[39] T.A. Silva, A. Wong, O. Fatibello-Filho, Electrochemical sensor based on ionic liquid and carbon black for voltammetric determination of Allura red colorant at nanomolar levels in soft drink powders, Talanta 209 (2020) 120588, https://doi.org/10.1016/j.talanta.2019.120588.

[40] M.R. Tomei, F. Arduini, D. Neagu, D. Moscone, Carbon black-based disposable sensor for an on-site detection of free chlorine in swimming pool water, Talanta 189 (2018) 262–267, https://doi.org/10.1016/j.talanta.2018.07.005.

[41] W.T.P. dos Santos, H.M.A. Amin, R.G. Compton, A nano-carbon electrode optimized for adsorptive stripping voltammetry: application to detection of the stimulant selegiline in authentic saliva, Sens. Actuators, B Chem. 279 (2019) 433–439, https://doi.org/10.1016/j.snb.2018.10.037.

[42] A.J. Bard, L.R. Faulkner, Electrochemical Methods: Fundamentals and Applications, 2nd ed., John Wiley & Sons, New York, 2001 http://elib.tu-darmstadt.de/tocs/95069577.pdf.

[43] B. Song, Y. Zhou, H. Jin, T. Jing, T. Zhou, Q. Hao, Y. Zhou, S. Mei, Y. Lee, Selective and sensitive determination of erythromycin in honey and dairy products by molecularly imprinted polymers based electrochemical sensor, Microchem. J. 116 (2014) 183–190, https://doi.org/10.1016/j.microc.2014.05.010.

[44] M.L. Avramov Ivić, S.D. Petrović, D.Ž. Mijin, F. Vanmoos, D.Ž. Orlović, D.Ž. Marjanović, V.V. Radović, The electrochemical behavior of erythromycin A on a gold electrode, Electrochim. Acta 54 (2) (2008) 649–654, https://doi.org/10.1016/j.electacta.2008.07.010.

[45] J.Y. Peng, C.T. Hou, X.X. Liu, H.B. Li, X.Y. Hu, Electrochemical behavior of azithromycin at graphene and ionic liquid composite film modified electrode, Talanta 86 (2011) 227–232, https://doi.org/10.1016/j.talanta.2011.09.005.

[46] A. Pappa-Louisi, A. Papageorgiou, A. Zitrou, S. Sotiropoulos, E. Georgarakis, F. Zougrou, Study on the electrochemical detection of the macrolide antibiotics clarithromycin and roxithromycin in reversed-phase high-performance liquid chromatography, J. Chromatogr. B Biomed. Sci. Appl. 755 (1-2) (2001) 57–64, https://doi.org/10.1016/S0378-4347(00)00614-9.

[47] A. Mahmoudi, M. Tertiş, L.-M. Simon, A. Van Schepdael, S. De Francia, L.-M. Junie, R. Săndulescu, Correlated quantification using microbiological and electrochemical assays for roxithromycin determination in biological and pharmaceutical samples, Talanta 211 (2020) 120703, https://doi.org/10.1016/j.talanta.2019.120703.

[48] X. Song, T. Zhou, Q. Liu, M. Zhang, C. Meng, J. Li, L. He, Molecularly imprinted solid-phase extraction for the determination of ten macrolide drugs residues in animal muscles by liquid chromatography-tandem mass spectrometry, Food Chem. 208 (2016) 169–176, https://doi.org/10.1016/j.foodchem.2016.03.070.

[49] C. Lan, D. Yin, Z. Yang, W. Zhao, Y. Chen, W. Zhang, S. Zhang, Determination of six macrolide antibiotics in chicken sample by liquid chromatography-tandem mass spectrometry based on solid phase extraction, J. Anal. Methods Chem. 2019 (2019) 1–13, https://doi.org/10.1155/2019/6849457.

[50] J. Suwanrut, N. Chantipmanee, W. Kamsong, S. Buking, T. Mantim, P. Saetear, D. Nacapricha, Temperature-dependent schlieren effect in liquid flow for chemical analysis, Talanta. 188 (2018) 74–80, https://doi.org/10.1016/j.talanta.2018.05.055.

[51] L.V. de Faria, T.P. Lisboa, T.A. Matias, R.A. de Sousa, M.A.C. Matos, R.A.A. Munoz, R.C. Matos, Use of reduced graphene oxide for sensitive determination of sulfanilamide in synthetic biological fluids and environmental samples by batch injection analysis, J. Electroanal. Chem. 892 (2021) 115298, https://doi.org/10.1016/j.jelechem.2021.115298.

[52] ANVISA - Agência Nacional de Vigilância Sanitária, Farmacopeia Brasileira - volume 2, 2019.

[53] P. Rebelo, J.G. Pacheco, M.N.D.S. Cordeiro, A. Melo, C. Delerue-Matos, Azithromycin electrochemical detection using a molecularly imprinted polymer prepared on a disposable screen-printed electrode, Anal. Methods 12 (11) (2020) 1486–1494, https://doi.org/10.1039/C9AY02566A.

[54] O. Vajdle, V. Guzsvány, D. Škorić, J. Csanádi, M. Petković, M. Avramov-Ivić, Z. Kónya, S. Petrović, A. Bobrowski, Voltammetric behavior and determination of the macrolide antibiotics azithromycin, clarithromycin and roxithromycin at a renewable silver–amalgam film electrode, Electrochim. Acta 229 (2017) 334–344, https://doi.org/10.1016/j.electacta.2017.01.146.

[55] L.K. Bekele, G.G. Gebeyehu, Application of different analytical techniques and microbiological assays for the analysis of macrolide antibiotics from pharmaceutical dosage forms and biological matrices, ISRN Anal. Chem. 2012 (2012) 1–17, https://doi.org/10.5402/2012/859473.

[56] M.F. Zaater, Y.R. Tahboub, E. Ghanem, Determination and stability assessment of clarithromycin in human plasma using RP-LC with electrochemical detection, J. Chromatogr. Sci. 50 (2012) 763–768, https://doi.org/10.1093/chromsci/bms055.

[57] P. Landová, M. Vávrová, A new method for macrolide antibiotics determination in wastewater from three different wastewater treatment plants, Acta Chim. Slovaca. 10 (2017) 47–53, https://doi.org/10.1515/acs-2017-0008.

[58] O. Vajdle, V. Guzsvány, D. Škorić, J. Anojčić, P. Jovanov, M. Avramov-Ivić, J. Csanádi, Z. Kónya, S. Petrović, A. Bobrowski, Voltammetric behavior of erythromycin ethylsuccinate at a renewable silver-amalgam film electrode and its determination in urine and in a pharmaceutical preparation, Electrochim. Acta 191 (2016) 44–54, https://doi.org/10.1016/j.electacta.2015.12.207.

[59] M. Radičová, M. Behúl, M. Vojs, R. Bodor, A Vojs Staňová, Voltammetric determination of erythromycin in water samples using a boron-doped diamond electrode, Phys. Status Solidi Basic Res. 252 (2015) 2608–2613, https://doi.org/10.1002/pssb.201552245.

[60] J.L. Rufino, H.R. Pezza, L. Pezza, Flow-injection spectrophotometric determination of azithromycin in pharmaceutical formulations using p-chloranil in the presence of hydrogen peroxide, Anal. Sci. 24 (7) (2008) 871–876, https://doi.org/10.2116/analsci.24.871.

[61] S. Mohamoudi, H. Rashedi, F. Faridbod, A molecularly imprinted polymer (MIP)-based biomimetic potentiometric sensing device for the analysis of Clarithromycin, Anal. Bioanal. Electrochem. 10 (2018) 1654–1667.

[62] H. Wan, F. Zhao, W. Wu, B. Zeng, Direct electron transfer and voltammetric determination of roxithromycin at a single-wall carbon nanotube coated glassy carbon electrode, Colloids Surf. B Biointerfaces 82 (2) (2011) 427–431, https://doi.org/10.1016/j.colsurfb.2010.09.014.

[63] C.E.R. De Paula, V.G.K. Almeida, R.M. Borges, R.J. Cassella, Spectrophotometric determination of azithromycin in pharmaceutical formulations employing the reaction with alizarin, Rev. Virtual Quim. 11 (2019) 1081–1096. https://doi.org/10.21577/1984-6835.20190074.